Intelligent Diagnostics for Aircraft Hydraulic Equipment

Intelligent Diagnostics for Aircraft Hydraulic Equipment

Oliver Ritter[1], Gerko Wende[2], Rocco Gentile[3], Francesco Marino[4], Antonio Carlo Bertolino[5], Andrea Raviola[6], Giovanni Jacazio[7]

[1,2] *Lufthansa Technik, Hamburg, 22335, Germany*
oliver.ritter@lht.dlh.de
gerko.wende@ lht.dlh.de

[3,4,5,6,7] *Politecnico di Torino – Department of Mechanical and Aerospace Engineering, Torino, 10129, Italy*
rocco.gentile@polito.it
francesco_marino@polito.it
antonio.bertolino@polito.it
s191117@studenti.polito.it
giovanni.jacazio@polito.it

ABSTRACT

In aviation industry, unscheduled maintenance costs may vary in a large range depending on several factors, such as specific aircraft system, operational environment, aircraft usage and maintenance policy. These costs will become more noteworthy in the next decade, due to the positive growing of worldwide fleet and the introduction of more technologically advanced aircraft. New implemented technologies will bring new challenges in the Maintenance, Repair and Overhaul (MRO) companies, both because of the rising number of new technologies and high volume of well-established devices, such as Electro-Hydraulic Servo Actuators for primary flight control. Failures in aircraft hydraulic systems deeply influence the overall failure rate and so the relative maintenance costs. For this reason, overhaul procedures for these components still represents a profitable market share for all MRO stakeholders. Innovative solutions able to facilitate maintenance operations can lead to large cost savings.

This paper proposes new methodologies and features of the Intelligent Diagnostic system which is being developed in partnership with Lufthansa Technik (LHT). The implementation of this innovative procedure is built on a set of failure detection algorithms, based on Machine Learning techniques. This development requires first to bring together the results from different parallel research activities:

1. Identification of critical components from historical data
2. Designing and testing automatic and adaptable procedure for first faults detection;
3. High-fidelity mathematical modeling of considered test units, for deeper physics analysis of possible failures;
4. Implementation of Machine Learning reasoner, able to process experimental and simulated data.

1. CRITICAL ISSUES IN MAINTENANCE OF AIRCRAFT EQUIPMENT

Cooper, Smiley, Porter, & Precourt (2017) predict an optimistic growth of commercial airline fleet. According to their report, in the next decade, the number of units will increase 3.4% net annually, rising the number of commercial aircraft more than 35000. This growing demand in both cargo and commercial fleets will be fulfilled on one hand introducing about 20000 new-generation aircraft and, on the other hand, replacing older units to about 10000 during this period (Figure 1). These numbers indicate that about 58% of the global aircraft fleet will include new-generation units and will radically influence many different technological issues. The presence of technologically advanced aircraft implies also considerable investments in MRO market. Cooper et al. (2017) report that “commercial airline MRO growth will be

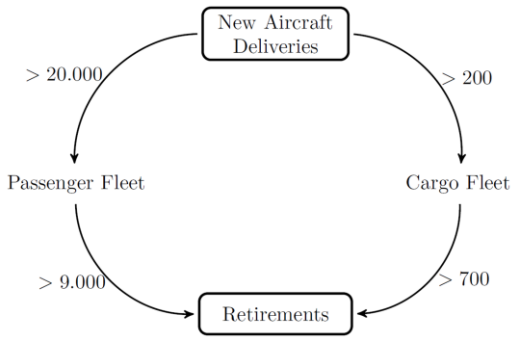

Figure 1: Global Aircraft Demand

healthy at 3.8% Compound Annual Growth Rate (CAGR) over the 10-year period, growing from the current demand of $ 75.6 billion to just over $ 109 billion by 2027". This rising investment expectation takes into account four main segments of MRO market: Airframe, Engines, Components and Line Maintenance. By the way, in order to improve the maintenance capability of these four sections, it is necessary to shift the paradigm at the base of the maintenance approach: from a reactive to a condition-based strategy. Both OEM players and MRO providers are dealing with new challenges related to new-generation fleet:

1. More sophisticated avionics components will require advanced health monitoring systems, which will be able to identify faults of the units;
2. The number of collected health-monitoring parameters will considerably rise, and all the MRO stakeholders have to find out what is the best way to take advantage from this amount of valuable data;
3. Line maintenance providers need to invest new capitals on both modern testing equipment and trainings about new health monitoring and fault isolation systems.

As reported by Groenenboom (2017), health-monitoring systems for aircraft were already regulated during the 1970s, when MSG-2 introduced the "Condition Monitoring" maintenance concept. During the last years, to improve their competitiveness in this field, also large MRO providers like Lufthansa Technik (LHT), Airfrance Industries and KLM Engineering & Maintenance have introduced their own health management and prognostic services. Today both OEMs and MRO providers aim to introduce health-monitoring innovative solutions able to facilitate maintenance operations that can lead to large cost savings. Mornacchi, Vachtsevanos and Jacazio (2015) indicated two areas that can benefit from an efficient health-monitoring system:

1. Improvement of aircraft operation reliability and dispatch-ability by avoiding on ground immobilization time and flight delays or re-routing or cancellations;
2. Reduction of direct maintenance costs by rescheduling maintenance operations, improving failures troubleshooting and performing maintenance tasks of anticipated failures;

Two main critical issues that negatively influence both cost areas are:

1. No Fault Found (NFF) cases: high number of equipment are removed from the aircraft because of a wrong fault indication, even though they result fully serviceable. The NFF rate is on average about 1/6 of the total number of signaled faults, nevertheless some equipment can reach a NFF rate above 25%;
2. Difficulty in identifying the actual faulty component which are classified as Line Replaceable Units (LRU). These units are complex assembly consisting of several sub-assemblies, and the identification of the failed part is a task that often requires large effort and time (Byington, Watson, & Edwards, 2004). Furthermore, many of these LRUs are installed in parallel for redundancy (for example the Flight Primary Control Systems), so usually for safety reason both the devices are removed though only one is failed.

The goal of this paper is to describe the actual development of fault diagnosis system for a given class of aircraft equipment, to obtain a high-quality, faster and cost-effective maintenance procedure. The presented case study is focused on the flight control actuators. These units can still be considered a key point for cost saving of maintenance procedures for three main reasons:

1. The components of the hydraulic system give a significant contribution to the overall failure rate and hence to the total associated maintenance cost;
2. Large passenger aircraft in service are equipped with two or three hydraulic systems for safety reasons;
3. Hydraulic systems are predestinated to be equipped with more sensors or are already equipped with a huge variety of sensors that are very good usable for prognostic algorithms and methods;
4. Hydraulic technology is projected to be the most common solution in the next future for flight controls and landing gear of the new versions of these large passenger aircraft (Mornacchi et al., 2015). Moreover, the benefits gained from more efficient maintenance procedures will thus not be limited to legacy aircraft but could be applied to new platforms.

2. PROJECT OBJECTIVES, METHODOLOGY AND USE CASE

The contents of this article summarize one year of collaboration between Polytechnic of Turin and LHT, which is aimed to investigate and design new suitable health-monitoring procedures for primary flight control actuators. This task constitutes a key cost saving factor for two main reasons:

1. Considerable numbers of Shop Load Event (SLE);
2. OEM-built test procedures for fault detection and isolation are not cost-effective in terms of maintenance time.

On this basis, the definition of a new automatic procedure could represent a remarkable advantage. An automatic procedure combined with an algorithm capable of detecting failures can really improve the overall maintenance quality. Marino (2017) reports that it is worthy to choose components that are widely installed on today and next-generation aircraft, to obtain a significant impact on future savings. The choice of the prototyping unit is based on both technical and economic criteria:

1. Number of subcomponent of the unit and overall complexity of the assembly;

2. Number of records and unique SLE;
3. Maintenance Total Costs (Overhauling Costs);
4. Time Since Installation (TSI);

During this cooperation with LHT, the first important research goal is the development of a new condition detection algorithm.

Several different approaches for fault detection and identification have been already adopted by Karpenko, Sepehri and Scuse (2003) who have identified three possible families of algorithms: the first one is a model-based approach (Isermann, 2005), while the second and the third use Machine Learning techniques in two different ways. Bernieri, D'Apuzzo, Sansone and Savastano (1994) have trained a neural network to reproduce the dynamic behaviour of the system, while different other approaches have used Machine Learning algorithms as pattern classifiers in order to recognise failure modes directly from the data of the dynamic system (Byington et al., 2004; Crowther, Edge, Burrows, Atkinson, & Woollons, 1998; Garimella & Yao, 2004; Le, Watton, & Pham, 1998; Mornacchi et al., 2015).

To make the last approach efficient, it is necessary to collect results from different engineering areas:

1. Techniques of data manipulation, state detection and identification of degradation;
2. Measurement campaigns of in-service components, both in healthy and degraded conditions;
3. High fidelity mathematical modeling of physical systems and mathematical description of fault propagation physics;
4. Data Mining and Data Fusion of historical, simulated and experimental results;
5. Implementation of Machine Learning Algorithms for processing data with the knowledge of physics of failure.

3. ANALYSIS OF MOST RECURRENT FAILURES

Once the reference unit has been identified, a further investigation is needed to recognize which sub-assemblies of are the most critical. This kind of analysis is also crucial for the implementation of an excitation signal that can be used to detect the most recurrent failures. The scheme in Figure 2 displays all the sub-assemblies of the reference Electro Hydraulic Servo-Actuator (EHSA). In the hydraulic part of the scheme, it is possible to distinguish:

1. Electro-Hydraulic-Servo-Valve (EHSV): jet-deflector kind where the first stage receives the current command by the external controller as input and it moves the deflector according to the rotation of the torque motor. This movement creates a pressure drop at the end of the second stage spool, which drives the correct flow to the cylinder chambers;
2. Symmetrical actuator: the position of the ram is determined by the difference of pressure between its two control chambers;
3. Mode Switching Valve (MSV): central valve controlled by two normally opened Electro-valves (EVs), which are placed in series, constituting a logic NOR function. This component is used to deactivate the unit and to set its function in damping mode. When both the two EVs are not activated, the spool of the MSV is directly connected with the supply line: in this way, the pressure force pushes the spool against its contrasting spring and the oil flows to the cylinder. If at least one of the EVs is turned on, the MSV spool is connected to the return line, and the EHSV is then bypassed (bypass-mode). The cylinder chambers are connected through a calibrated orifice which is responsible of damping action.
4. Accumulator: this component supplies flow to avoid pressure to drop below the cavitation value and, in case of hydraulic supply interruption, it allows the actuator rod to come back in its neutral position.

The control part of the scheme includes a position sensor for closed loop position and a Mechanical Recentering Device which mechanically connects the linear ram with the spool of the EHSV. This security component moves the main ram in its null position in case of electrical failure of the current supply in the first stage of the EHSV. All these main sub-assemblies contain several other components that can be substituted in case of failures. The information about the replaced parts are recorded during each SLE. These records constitute an historical database of all the replaced components of each adjusted sub-assembly which represents a valuable tool for the analysis of the most recurrent exchanged parts during repairing operations.

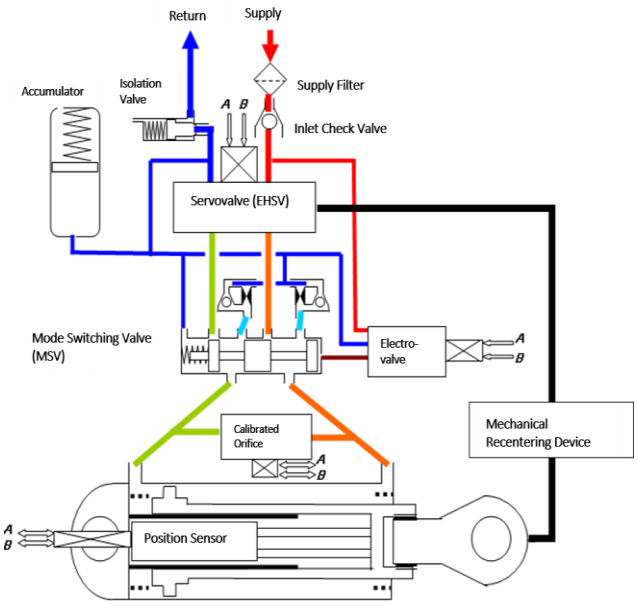

Figure 2: EHSA reference configuration

The results of this investigation have shown that some sub-assemblies like the electro-valves or the mechanical feedback are less critical than others, like the EHSV, that is the most exchanged component. This classification can be considered a first guideline for the definition of the excitation signal, first step of the Intelligent Diagnostic procedure.

4. IMPLEMENTATION OF INTELLIGENT DIAGNOSTIC

As first step of the implementation of an Intelligent Diagnostic, the definition of an automatic failure-recognition procedure has an important impact in terms of cost saving of standard maintenance procedure. The base of this development is a specific command sequence that can identify in a short time the most recurrent failures in the critical subcomponents. In this way, it would be possible to substitute the standard maintenance procedure with a fast and efficient self-designed Entry Test. Indeed, standard test procedures contain specific commands to assess the performance of the subassemblies in the EHSA, but these procedures can last hours, and they must be performed at least two times (one for the Entry and one for the Certification Test). This approach is not considered time and cost-effective anymore. The main advantages of an automatic command sequence can be synthetized:

1. Automation: Entry Test can run automatically without any human-interaction during the measurements in a short period of time, while all the needed Health Features (HF) can be collected;
2. Standardization: since there are no interactions with the operator during the duration of the test, the measured time responses are always the same. This means that is possible to compare the responses and increase the knowledge about similar cases;
3. Continuous measurement: it is possible to collect data about physical parameters during the entire command sequence;
4. Scalability of the test procedure: since the main components of several primary flight control actuators are the same, the designed automatic procedure for the reference unit can be adapted to other kind of actuators.

During the design of this automatic entry test, both the classification the most critical sub-assemblies and the historical data of the most recurrent failed certification tests have been considered. With this automatic procedure, it will be possible to collect a large number of data. This database with all the possible historical collected measurements of degraded and healthy units will considerably enlarge the knowledge of all the single degradations in the EHSA, constituting the base for the development of a Machine Learning algorithm for fault detection. By the way, this database would require long-lasting measurement and data collection campaigns. This issue can be overcome increasing the number of samples with simulated data through a high fidelity mathematical model. This development strategy can be classified as a combination of Model Based and Data-Driven approaches, similarly as the Hybrid Diagnosis Approach for Electro-mechanic Actuators (Narasimhan, Roychoudhury, Balaban, & Saxena, 2010).

5. MATHEMATICAL MODELING AND SIMULATIONS

The most important advantage of a model-based approach is its flexibility: in a highly-detailed physical model, it is possible to set a wide range of possible degradations, with any kind of severity. The more complex and detailed the model is, the more number of possible case studies increases. Using the same approach of Bertolino, Jacazio, Mauro and Sorli (2017), the final goal of high-fidelity model is to create a virtual bench that can replicate the nominal behavior of the physical unit and to "evaluate its behavior correlating it with small variations" of some parameters, corresponding to physical characteristic of the unit. This strategy allows to have a greater flexibility on studying the effects of several flaws injection combinations, due to the absence of hardware. Although it speeds up the failure physics investigation, it represents an issue as well: indeed, the model has first to be validated and tuned on real measurements.

5.1. Model Structure

The high fidelity dynamic non-linear model has been developed in Matlab - Simulink® environment and it is the evolution of the model developed by Mornacchi (2016). Its structure can be divided in three conceptual layers (Figure 3):

1. First Layer contains all the necessary data to introduce different degradations in terms of severity and starting time;
2. Second Layer includes three sub-files with not only physical characteristics of EHSA itself, but also the ones of its seals and used fluid;
3. Third Layer contains all the files concerning the real physical modeling of the unit. Inside the cardinal EHSA blocks in Figure 3 all the physical components in Figure 2 are modelled with a white-box approach.

The entire model is physically meaningful and each component motion is determined by the resolution of d'Alambert differential dynamic equations, as in Bertolino et al., 2017. The behavior of these inner EHSA parts are influenced by all the other blocks in Layer 3. *Command* block contains the same excitation-signal that has been adopted for the experimental campaign, and it interacts with *Oil Properties* and *Test Bench* blocks. In particular, the latter is the only component that has not been modelled in a physical way, in order to not considerably increase the overall complexity. A Discrete- time Autoregressive Exogenous model (ARX) has been adopted because it results particularly suitable for modelling "dynamic process driven by and input in presence of uncertainties" (Diversi, Guidorzi, & Soverini,

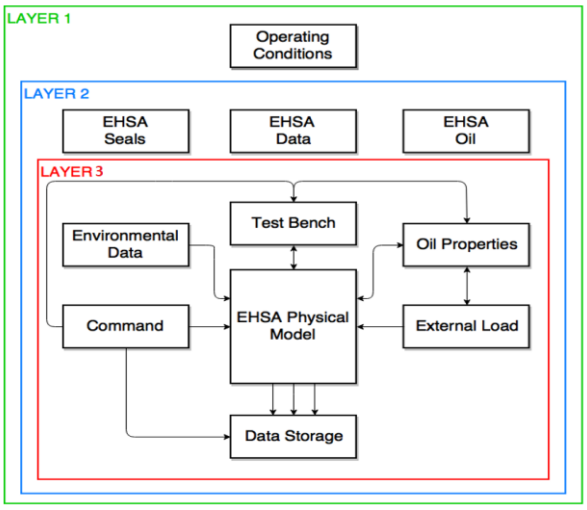

Figure 3: Simulink Model Conceptual Structure

2010). The connection between EHSA and external environment is controlled by the blocks *Environmental Data* and *External Load*, which is deactivated at the moment because any load test has been carried out so far. When a simulation is completed, the *Data Storage* block collects all the useful data for post-processing and further analysis. In the next paragraphs, the models of the EHSA sub-assemblies will be briefly described, and at the end a comparison between experimental and simulation results will be shown.

5.2. EHSA Main Ram

The hydraulic main ram is a 2DOF (Figure 4) model where:

1. $x_R, \dot{x}_R$ and $\ddot{x}_R$ are position, velocity and acceleration of the ram;
2. $x_C, \dot{x}_C$ and $\ddot{x}_C$ are position, velocity and acceleration of the external sleeve structure;

The external damper C_{ext} corresponds to the external eye-end of the ram, and it results particularly useful in case of external load F_{ext}. As mentioned in the previous paragraph, all the simulations have been performed without any external acting force. C_{sa} and K_{sa} represent the damping coefficient and the stiffness of the external connection between the sleeve and the fixed frame. Both in these points and in the ram end, it is possible to include the effect of backlash, following the approach of Bertolino (2016); Bertolino et al. (2017); Martin, Jacazio and Vachtsevanos (2017) and Nordin, Galic and Gutman (1997). The main ram receives as input the control flows from the EHSV, through the MSV (Q_1 and Q_2) and it returns as output both its position and the external sleeve one (x_R and x_C). The difference between them is the relative displacement of the ram and it is used to close the position control loop. The pressures in both the chambers p_1 and p_2 are calculated as function of the volumetric flow rates, the fluid properties and the geometric characteristics. In order to simulate also the seals failures, Q_1 and Q_2 are affected by two different types of leakages: internal between the chambers (Q_{li}) and external between the chambers and outside (Q_{lei}). Continuity equations in both the chambers can be written as:

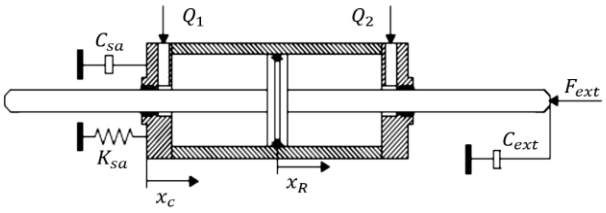

Figure 4: Actuator Model Scheme

$$\frac{\partial p_1}{\partial t} = \beta \frac{Q_1 - Q_{le1} - Q_{li} - (\dot{x}_R - \dot{x}_C)A}{V_0 + x_R A} \quad (1)$$

$$\frac{\partial p_2}{\partial t} = \beta \frac{Q_2 - Q_{le2} + Q_{li} + (\dot{x}_R - \dot{x}_C)A}{V_0 - x_R A} \quad (2)$$

where β is the oil bulk module, V_0 is the initial volume of the chambers when the ram is centered and A represents the surface of the head of the piston. The results of Eq. (1) and Eq. (2) are then used to determine the position of ram and sleeve according to the following dynamic equations:

$$m_R \ddot{x}_R = (p_1 - p_2)A - \gamma(\dot{x}_R - \dot{x}_C) - F_{fric} - C_{ext}\dot{x}_R \quad (3)$$

$$m_C \ddot{x}_C = (p_2 - p_1)A + \gamma(\dot{x}_R - \dot{x}_C) + F_{fric} - C_{sa}\dot{x}_C - K_{sa}x_C \quad (4)$$

where m_R and m_C are the masses of the ram and the sleeve respectively, γ is the viscous friction coefficient and F_{fric} stands for the Coulomb friction force. In particular, the model of friction allows both the static and dynamic conditions and the switching between them to be considered. Static friction value is evaluated according to the pressure in both the chambers and the geometrical and physical data of the seals (Martini, 1984). The dynamic value instead and the condition of commutation are modeled as described in Bertolino (2016) and Bertolino et al. (2017).

5.3. Servo-valve EHSV

The EHSV is the most critical and complex component of both the model and real unit. It represents the interface component between the control logic and the hydraulic part and its behavior influences the entire dynamic response of the actuator. The real installed servo-valve in the unit is a jet-deflector, whereas the simulated one is flapper-nozzles type. This difference is only in the first stage of the EHSV and it does not influence the dynamic response or the reliability of the global physical model of the actuator. The inner structure of both the types can be divided in:

1. First stage: it transforms the electrical input into a low power hydraulic signal. It includes the torque motor and flapper dynamics. The torque motor block receives as input the current i_{com} coming from the controller,

whereas the flapper dynamic gives as output the position of the flapper x_f ;

2. Second Stage: it transforms the low power hydraulic command signal into a high power hydraulic flow. It contains the blocks of the hydraulic amplifier and spool dynamics. According to the flapper position, the hydraulic amplifier block evaluates the difference of pressure between the command chambers of the sleeve Δp_{spool}, that controls the final position of the spool x_s.

The model of the torque motor is based on the magnetic circuit analyzed by Urata (2007), where the sources of magnetic forces are the permanent magnets V_p and solenoid magnetic force ni_{com} (Figure 5). Each reluctance in the circuit is calculated taking into account the air-gap thickness, and eventual misalignment of the armature. The generated torque is expressed considering the magnetic fluxes through the air-gaps:

$$T = \frac{L_a A_g}{4\mu_a} \sum_{i=1}^{4} B_i \tag{5}$$

where B_i is the flux density between the four air gaps between magnet and solenoids, L_a is the distance between the left and right pole, A_g is the cross-sectional area of the air-gap and μ_a is magnetic permeability of the air. At the end of the first stage of the EHSV; x_f is calculated combining the Eq. (5) with the dynamic rotation equation of the torque motor anchor. The position of the flapper determines the difference of pressure between the chambers of the sleeve, regulating the flow through the nozzle channels. These pressures are function of both x_f and spool velocity:

$$p_A = G_P \left(x_f - \frac{A_{spool}}{G_Q} \dot{x}_s \right) \tag{6}$$

$$p_B = -G_P \left(x_f - \frac{A_{spool}}{G_Q} \dot{x}_s \right) \tag{7}$$

where G_P and G_Q are respectively pressure and flow gain. The imbalanced pressure $\Delta p_{spool} = p_A - p_B$ on the two-side spool creates a displacement that allows the flows to run

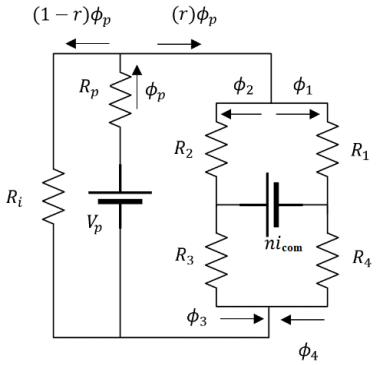

Figure 5: Magnetic Torque Motor Circuit (Urata, 2007)

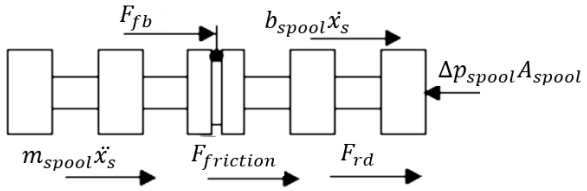

Figure 6: EHSV Spool Free Body Diagram

through the actuator chambers. The equation of the free body diagram in Figure 6 takes into account the force of the feedback spring F_{fb}, which connects the flapper with the spool, the Recentering Device equivalent force F_{rd} (section 5.5), Coulomb and viscous friction forces and structural damping. Since there are not seals, the dynamic friction is a constant value and does not follow the laws proposed by Martini (1984). Once x_s is determined, it is necessary to evaluate the flow through each port of the EHSV, considering both supply and return contributes. This issue is modelled with an equivalent Weathstone circuit (Merritt, 1967), where each port is represented as a variable resistance with two components in series: a laminar term R_C and a turbulent one R_A (Mornacchi et al., 2015). Once these values are evaluated for all the control ports, the model calculates the flow through each control port through Eq. (8).

$$Q_{SV} = \frac{-R_C + \sqrt{R_C^2 - 4R_A|\Delta p_{spool}|}}{2R_A} * sgn(\Delta p_{spool}) \tag{8}$$

5.4. Mode Switching Valve MSV

Physically the dynamic of the spool of the MSV is similar to the second stage of the EHSV, without any feedback force F_{fb} but with an elastic force from its contrasting spring. It is connected not only to the EHSV, but also with the accumulator and the orifice between the chambers in case of damping mode. It can reach just two discrete positions (opened or closed) and it can be commanded by just one of the two installed EVs. Once the position of the MSV is determined, the flows through its ports can be determined considering both laminar and turbulent flow resistances, as for the EHSV.

5.5. Recentering Device RD

Particularly relevant component in both normal and unexpected working conditions of the unit. It consists of a complex mechanical device which moves the main ram to its null position in case of failure of the current supply to the EHSV. It is both connected to the main ram and to the jet deflector system of the EHSV (equivalent to the flapper of the flapper-nozzles valve), as shown in the diagram of Figure

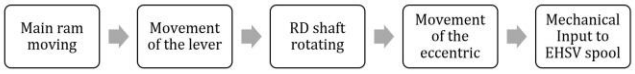

Figure 7: Recentering Device Block Scheme

7. One side of the main ram is linked to the RD rotating shaft hinge on which is mounted the RVDT transducer. The rotation of this component moves a small eccentric cam that directly controls the motion of the jet deflector system inside the EHSV, thanks to two contrasting springs. This mechanical effect is compensated directly by the external controller, which provides to the EHSV an additional offset current both in extension and retraction. By the way, this offset is not constant for the entire stroke, but the RD works as nonlinear force that depends on the position of the main ram. Since its geometry is complex, the effect of this component is considered inside the model through its zero order characteristic curve. Its offset effect has been considered with an equivalent force F_{rd} on the EHSV spool (Figure 7).

5.6. Test Bench TB

As already mentioned in 5.1, the dynamic model of the TB is built with an ARX Model, because most of the physical parameters are unknown and in order to reduce the complexity of the model. Model tuning is performed using two different sets of measured data: supply pressure and outlet flow. Part of these two time-series (70% of the time-span of the command) is used for the model identification, while the remaining part for its validation. The equation at the base of an ARX model is:

$$A(q)y(t) = B(q)u(t - n_k) + e(t) \quad (9)$$

where $q(t)$ is a delay operator, $e(t)$ is a white noise, n_k represents delay from input to output in terms of number of samples and $A(q)$ and $B(q)$ are two linear functions defined as follow:

$$A(q) = 1 + a_1 q^{-1} + \cdots + a_{n_a} q^{-n_a} \quad (10)$$

$$B(q) = b_1 + b_2 q^{-1} + \cdots + b_{n_b} q^{-n_b+1} \quad (11)$$

where:

1. $y(t)$: model output at instant t;
2. n_a: number of poles, so the number of past output terms to predict the current output;
3. n_b: number of zeros plus one, so the number of past input terms to predict the current output;

In this case, the best fitting is obtained fixing $n_a = nb = 4$ and $n_k = 0$, with a reached accuracy of more than 95%. The

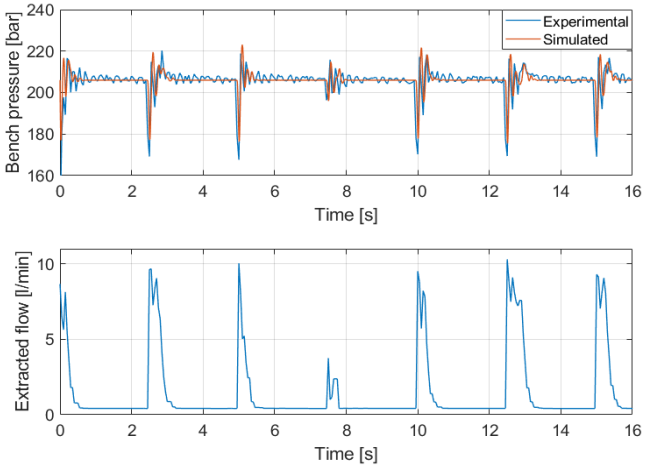

Figure 8: Pressure drop comparison between simulated and experimental results

plots in Figure 8 displays a comparison between measured and simulated supply pressure commanding the unit with a Pseudorandom Binary Sequence (PRBS) in closed loop, with reference to the input extracted flow.

5.7. Model Validation

The model validation is performed using data acquired during the experimental campaign at Lufthansa Technik facilities. The plots in Figure 9-left) displays a comparison between measured and simulated position and EHSV current during the PRBS sequence. A closer look in the 30th second in Figure 9-right) shows that the outputs of the model are very close to the actual behavior, concerning both the current of EHSV and the main ram position. Both the plots show that the model is able to represent in an accurate way the system behavior and that it can be used to study the performance degradation when the parameter values move away from the baseline condition.

6. DATA ANALYSIS AND EARLY STAGE DEVELOPMENT OF MACHINE LEARNING ALGORITHM

As previously anticipated, a crucial point within the Intelligent Diagnostic frame is the development of a Machine Learning Algorithm for fault classification. The idea is to develop an algorithm which provides a unique and accurate indication of where the failure is located in the EHSA, by using the features extracted from the raw signals acquired during the initial automatic Entry Test. The development of this specific part of the Intelligent Diagnostic presents some critical issues:

1. Number of entries reported inside historical database;
2. Some reports could not present all the needed information for this investigation;

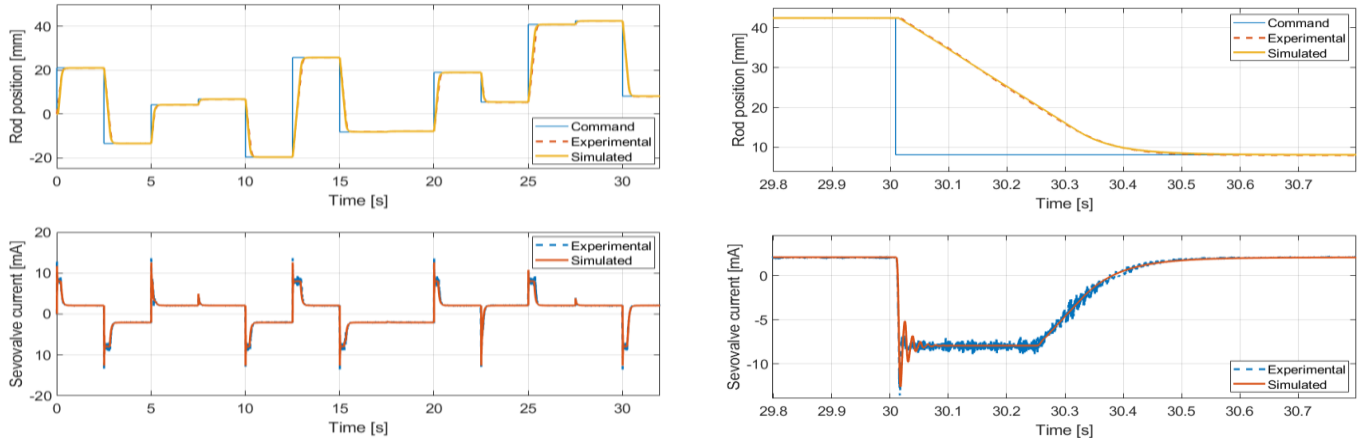

Figure 9: Left) Model and Experimental Results – PRBS Test; Right) Particular of previous graph on the left side

3. Difficulties in disambiguation of some physical degradations that affect the EHSA response in similar ways.

As already mentioned in paragraph 3, the analysis of historical data of repairing reports indicates the EHSV as most recurrent exchanged sub-assembly. Furthermore, this part can be considered as the most complex and crucial element for the correct behavior of the EHSA. From data-mining perspective, the large number of entries in the database (70% of the recorded SLEs) guaranties a good starting database for fault identification. Despite the large number of events, the information related to the health status of the EHSV are just two since the EHSV can be entirely replaced or not. As consequence, an initial binary classification can be easily achieved as first step to prove the feasibility of the ML development. According to what reported above, the historical information regarding the EHSV were classified in two classes, marked with a binary label: zero if the sub-assembly needs to be replaced, or one otherwise.

6.1. Database Generation

In order to increase the number of entries, the historical database has been combined with simulated results, created including EHSV degradations. The first step for building this database is to evaluate how many HF are directly related to the EHSV behavior. From this result, the historical database of SLE has been "cleaned" from useless data:

1. Data loss due to missing information;
2. All the features not directly linked to the EHSV.

In order to increase the database size, several hundred simulated responses have been performed with different combinations of EHSV degradation. Five different possible physical degradations were considered with different levels of severity and considered in pair:

1. Excessive roundness of control ports orifice due to local wears, which can have important impact on the control flows;
2. High hysteresis current in the first-stage torque motor;
3. Increase of radial clearance between spool and sleeve;
4. Stiffness variation of the feedback spring between first and second stage;
5. Excessive backlash between feedback spring and spool;

These simulated degradations can be directly detected extracting the health-features directly from the EHSA response of six specific portions of the complete excitation signal. In particular, these parts of the signal include all the standard certification tests that are strictly influenced by the EHSV behavior. These six signals have been used as input of the Simulink Model and, from the analysis of its responses, eighteen Health Features (HF) have been extracted as output. If either one of them results out of standard test limits, the troubleshooting of the related test would be to substitute the failed EHSV, and the entire entry-simulated test would be not passed. An example of the structure of the built database is shown in Table 1: the first eighteen columns represent the extracted health features from the signal. The last column "Label" reveals the final result of the entry test: one if all the health features are within their limits, and zero if at least one test is not passed. Finally the historical and simulated results were merged together in one database. The database structure, as reported in Table 1 constitutes the training dataset used to implement the supervised ML algorithm for binary classification between those unserviceable sub-components and the serviceable ones.

	HF n.1	HF n.2	…	HF n.18	Label
Actuator 1	…	…	…	…	1
Actuator 2	…	…	…	…	0
…	…	…	…	…	
Actuator n-th	…	…	…	…	1

Table 1: Database Structure of the Simulated Extracted Health Features

6.2. Implementation of Neural Network for Failure Classification

The implemented ML algorithm for this binary classification is a supervised Neural Network (NN), which has to be trained in order to detect data representing failure modes of the dynamic system. Chen and Burrell (2001) have already highlighted how NN can be particularly suitable for "pattern matching and classification problem". In this first stage of design, the Multilayer Perceptron (MLP) structure has been developed in order to perform a logistic classification between Failed and Passed units, as reported in the last columns of Table 1. This initial step of the ML algorithm has been fundamental for two main reasons:

1. It has demonstrated ability to recognize anomalous behaviors by learning from the provided data during the training stage;
2. It constitutes the first step for a more specific identification of the failure component inside the EHSV, while nowadays the entire servo-valve is completely removed without any further investigation.

The architecture of the proposed fault diagnostic algorithm is similar to the one in Figure 10: in this case, the NN presents eighteen input nodes, corresponding to the extracted HF, and two full dense hidden layers with forty nodes each. The final output layer contains just one node, which can assume binary values as reported in the Label column of Table 1.

Both the hidden layers employ a Rectifier Linear function (ReLu) as activation, whereas the last output layer adopts a sigmoid function because of its two possible binary states. During the training phase of the NN, to improve the way it learns, it is necessary to choose wisely:

- The Training Set of Data from the original database, where two balanced classes of passed and failed tests are represented equally;
- Its Loss Function $\mathcal{L}$ to better cope with NN learning slowdown;
- A Regularization Method, "which make our network better at generalizing beyond the training data" (Nielsen, 2017);
- The Network hyper-parameters, like the learning rate or the optimization parameters.

The Training Set has been extracted from the HF database in Table 1. However, these features are of different type and scale, so before feeding them inside the input layer, they have been regularized with the standard scaler. The standard scaler regularization assumes that the data are normally distributed and scale the result in a way that the distribution would be centered on zero, with a standard deviation of one:

$$\tilde{x}_i = \frac{x_i - mean(x)}{stdev(x)} \tag{12}$$

where x represents a feature and i indexes the i^{th} training sample. Once the dataset is normalized it is possible to split randomly the entire database into: training set and test set, with a ratio of 4:1. This sub-set of data for training has to be as much balanced as possible, in order to prevent the algorithm from overfitting the dataset, which would then affect in a negative way the classification performance. The loss function used ($\mathcal{L}$) is a particular case of the multinomial cross-entropy loss where each example belongs to a single class, particularly suitable for binary classification:

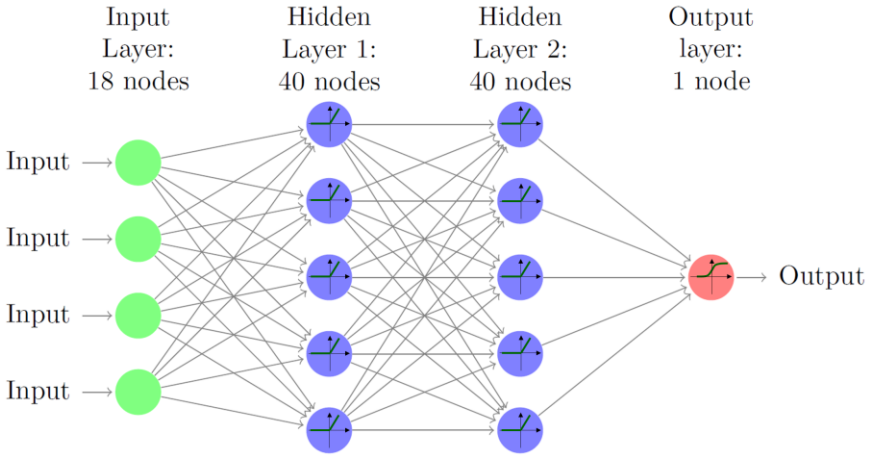

Figure 10: Neural Network Structure

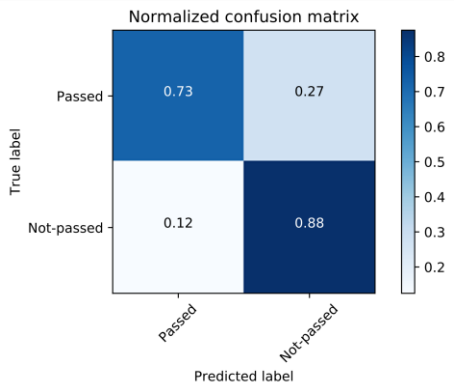

Figure 11: Normalized Confusion Matrix

$$\mathcal{L} = -\frac{1}{n}\sum_{i=1}^{n}[y_i\, log(p_i) + (1-y_i)\, log(1-p_i)] \qquad (13)$$

where i indexes the samples, y is the sample label and p is the prediction for a sample. Once the structure of the algorithm is defined it is required to tune all the hyper-parameters of the NN. Large NN requires a considerable number of free parameters, which need to be accurately selected and evaluated during the training to maximize the metric score considered but also to make the NN generalize and properly working with a new set of inputs. Dropout is a regularization technique for addressing this overfitting problem. The key idea is to randomly drop neurons (along with their connections) from the NN during training to prevent units from co-adapting too much. In this way, every time that a new training input is set as input, the NN presents a different shape, but at the end "all these architectures shares weights" (Krizhevsky, Sutskever, & Hinton, 2012). At test time, the drop of the unit is not performed and predictions of all these sub-structures compose a NN that has smaller weights. In our specific case, the dropout parameter has been settled to 0.6 (likelihood of keeping a specific neuron active). The training of the NN has been performed with the backpropagation approach with the Adaptive Moment Estimation optimization algorithm (Kingma & Ba, 2015). This optimization method computes the adaptive learning rates for each parameter and stores the exponential decaying average of the past squared gradients. Finally, the metric used to score the algorithm was the accuracy. The Accuracy achieved by using the algorithm is about 80% of correct classification (Figure 11):

$$Accuracy = \frac{\sum True\ positive + \sum True\ negative}{\sum Total\ population} \qquad (14)$$

This level of accuracy proves the feasibility of this method that can be extended starting from the EHSV to many other subcomponents of the actuator. To improve the accuracy is then possible both to increase the number of samples with simulated data and improve the quality of the features used to perform the classification. Furthermore, as already mentioned in the beginning of the paragraph, this algorithm constitutes the first base for a more complex NN architecture for the localization of the failure inside the EHSV. These further steps will be achieved in the next future to improve the accuracy level and ensure a better diagnostic level.

7. CONCLUSION

This paper summarizes the current development for a new and Intelligent Diagnostic methodology for primary flight control systems. The combination between an automatic failure-recognition procedures, simulated results with High-Fidelity Mathematical Model and Machine Learning algorithm for failure localization are already providing excellent results in terms of time and cost savings.

Further improvements of this research will involve all three main topics of the research:

1. Extension of the automatic procedure to other different primary flight control systems, following the same methodology used for the reference EHSA;
2. Starting from the current results with failures in the EHSV, the simulation campaign will be widened, including more induced local faults in other sub-assemblies. An interesting study will include the analysis of the unit behavior combining faults in different sub-assemblies;
3. Accurate management of all the collected data from real and simulated results, in order ensure a reliable and high diagnostic level from the Machine Learning algorithm. The final goal will be to provide a tool which is able not only to classify if the tested unit is serviceable or not, but also to localize the defected component inside the affected sub-assembly of the EHSA.

ACKNOWLEDGEMENT

This work was supported by Lufthansa Technick AG. We appreciate their contribution to the development and validation of the mathematical model by providing to the research team important data, actuators and technology applied to test bench.

NOMENCLATURE

A	Surface of the Head of the Piston
A_g	Cross-Sectional Area Air-Gap
A_{spool}	Spool Section Area
B_i	Flux Density in i-th Air Gap
C_{ext1}	Damping Coefficient of Ball-eye of the Actuator
C_{sa}	Damping Coefficient of External Sleeve Structure
CAGR	Compound Annual Growth Rate

EHSA	Electro- Hydraulic Servo Actuator
EHSV	Electro- Hydraulic Servo Valve
F_{fb}	Feedback-spring Force
F_{fric}	Coulomb Friction Force
F_{rd}	Recentering Device Force on the EHSV spool
G_P	EHSV Pressure Gain
G_Q	EHSV Flow Gain
HF	Health – Features
K_{sa}	Stiffness of External Sleeve Structure
L_a	Distance between Magnetic Poles
LHT	Lufthansa Technik
LRU	Line Replaceable Unit
MRO	Maintenance Repair and Overhaul
MSV	Mode Switching Valve
NARX	Nonlinear Autoregressive Exogenous Model
NFF	No Fault Founds
NN	Neural Network
OEM	Original Equipment Manufacturer
Q_1, Q_2	Control Flows in the Actuator Chambers
Q_{li}	Internal Leakage Flow between Actuator Chambers
Q_{le}	External Leakage Flow of i-th Chamber
R_C, R_A	Laminar and Turbulent Resistance in EHSV ports
RD	Recentering Device
SLE	Shop Load Event
T	Torque applied by the EHSV Torque Motor
TSI	Time Since Installation
V_0	Initial Volume of both Actuator Chambers
i_{com}	Command Current
m_R	Mass of the Actuator Ram
m_C	Mass of the Actuator Sleeve
p_1, p_2	Pressures in the Actuator Chambers
p_A, p_B	Pressures in the EHSV Spool Chambers
x_C	Displacement of the Actuator Sleeve
x_f	Flapper Position
x_R	Position of the Actuator Ram
x_s	Spool Position
Δp_{spool}	Pressure Drop between EHSV Sleeve Chambers
β	Oil Bulk Module
γ	Viscous Friction Coefficient
μ_a	Air Magnetic Permeability

REFERENCES

Bernieri, A., D'Apuzzo, M., Sansone, L., & Savastano, M. (1994). A neural network approach for identification and fault diagnosis on dynamic systems. *IEEE Transactions on Instrumentation and Measurement*, *43*(6), 867–873. https://doi.org/10.1109/19.368083

Bertolino, A. C. (2016). *Modellazione di Sistema Vite/Madrevite in Attuatori Elettromeccanici per Comandi di Volo*. Politecnico di Torino. Retrieved from http://www.informaworld.com/openurl?genre=article&doi=10.1080/03043798408903597&magic=crossref%7C%7CD404A21C5BB053405B1A640AFFD44AE3

Bertolino, A. C., Jacazio, G., Mauro, S., & Sorli, M. (2017). High Fidelity Model of a Ball Screw Drive for a Flight Control Servoactuator. In *ASME 2017 International Mechanical Engineering Congress and Exposition* (pp. 1–10). Tampa, Florida, USA.

Byington, C. S., Watson, M., & Edwards, D. (2004). Data-driven neural network methodology to remaining life predictions for aircraft actuator components. In *IEEE Aerospace Conference Proceedings* (Vol. 6, pp. 3581–3589). https://doi.org/10.1109/AERO.2004.1368175

Chen, D., & Burrell, P. (2001). Case-Based Reasoning System and Artificial Neural Networks: A Review. *Neural Computing & Applications*, *10*(3), 264–276. https://doi.org/10.1007/PL00009897

Cooper, T., Smiley, J., Porter, C., & Precourt, C. (2017). *Global Fleet & MRO Market Forecast Summary*. Retrieved from http://www.oliverwyman.com/our-expertise/insights/2016/apr/mro-survey-2016.html

Crowther, W. J., Edge, K. A., Burrows, C. R., Atkinson, R. M., & Woollons, D. J. (1998). Fault diagnosis of a hydraulic actuator circuit using neural networks—an output vector space classification approach. *Proceedings of the Institution of Mechanical Engineers, Part I: Journal of Systems and Control Engineering*, *212*(1), 57–68. https://doi.org/10.1243/0959651981539299

Diversi, R., Guidorzi, R., & Soverini, U. (2010). Identification of ARX and ARARX models in the presence of input and output noises. *European Journal of Control*, *16*(3), 256–257. https://doi.org/10.1016/S0947-3580(10)70649-X

Garimella, P., & Yao, B. (2004). Fault detection of an electro-hydraulic cylinder using adaptive robust observers. In *2004 ASME International Mechanical Engineering Congress and Expo*.

Groenenboom, J. (2017). Aircraft Health Monitoring: The True Value of Aircraft Health Monitoring and Data Management. In *13th Maintenanance Cost Conference*. Panama City.

Isermann, R. (2005). Model-based fault-detection and diagnosis - Status and applications. *Annual Reviews in Control*, *29*(1), 71–85. https://doi.org/10.1016/j.arcontrol.2004.12.002

Karpenko, M., Sepehri, N., & Scuse, D. (2003). Diagnosis of process valve actuator faults using a multilayer neural network. *Control Engineering Practice*, *11*(11), 1289–1299. https://doi.org/10.1016/S0967-0661(02)00245-9

Kingma, D. P., & Ba, J. (2015). Adam: A Method for Stochastic Optimization. In *ICLR: International*

Conference on Learning Representations (pp. 1–15). San Diego. https://doi.org/http://doi.acm.org.ezproxy.lib.ucf.edu/10.1145/1830483.1830503

Krizhevsky, A., Sutskever, I., & Hinton, G. E. (2012). ImageNet Classification with Deep Convolutional Neural Networks. *Advances In Neural Information Processing Systems*, 1–9. https://doi.org/http://dx.doi.org/10.1016/j.protcy.2014.09.007

Le, T. T., Watton, J., & Pham, D. T. (1998). Fault classification of fluid power systems using a dynamics feature extraction technique and neural networks. *Proceedings of the Institution of Mechanical Engineers. Part I: Journal of Systems and Control Engineering*, *212*(2), 87–97.

Marino, F. (2017). *Advanced Fault Detection and Classification on Primary Flight Control Actuators*. Polytechnic of Turin.

Martin, A. De, Jacazio, G., & Vachtsevanos, G. (2017). Windings Fault Detection and Prognosis in Electro-Mechanical Flight Control Actuators Operating in Active-Active Configuration. *International Journal of Prognostics and Health Management*, (1991), 0–13.

Martini, L. J. (1984). *Practical Seal Design*. (T. & Francis, Ed.).

Merritt, H. E. (1967). *Hydraulic Control Systems*. (I. John Wiley & Sons, Ed.). New York, London, Sydney: John Wiley & Sons, Inc.

Mornacchi, A. (2016). *Design and Development of Prognostic and Health Management System for Fly-by-Wire Primary Flight Control Electrohydraulic Servoactuators*. Politecnico di Torino.

Mornacchi, A., Vachtsevanos, G., & Jacazio, G. (2015). Prognostics and Health Management of an Electro-Hydraulic Servo Actuator. In *Annual Conference of the Prognostic and Health Management Society* (pp. 1–12).

Narasimhan, S., Roychoudhury, I., Balaban, E., & Saxena, A. (2010). Combining Model-Based and Feature-DrivenFeature-Driven Diagnosis Approaches – A Case Study on Electromechanical Actuators. In *21st International Workshop on Principles of Diagnosis* (pp. 1–9). Retrieved from https://ntrs.nasa.gov/search.jsp?R=20110008515

Nielsen, M. (2017). Improving the Way Neural Network Learnitle. Retrieved from http://neuralnetworksanddeeplearning.com/chap3.html

Nordin, M., Galic', J., & Gutman, P.-O. (1997). New models for backlash and gear play. *International Journal of Adaptive Control and Signal Processing*, *11*(1), 49–63. https://doi.org/10.1002/(SICI)1099-1115(199702)11:1<49::AID-ACS394>3.0.CO;2-X

Urata, E. (2007). Influence of unequal air-gap thickness. In *Proceedings of the Institution of Mechanical Engineers, Part C: Journal of Mechanical Engineering Science* (Vol. 221, pp. 1287–1297).

BIOGRAPHIES

Oliver Ritter, graduated in Mechanical Engineering at the Institute of Aircraft Systems Engineering of the Technical University of Hamburg in 2013. After graduation he directly started as a Project Engineer at the Lufthansa Technik Base in Hamburg. As an EASA 21-J Design Engineer Oliver Ritter has gained relevant experience in research and innovation projects at the components division of Lufthansa Technik. The focus of his engineering activities is the development and improvement of test equipment and procedures for flight control systems. For this purpose, Oliver Ritter is the responsible operator of a hydraulic test laboratory, where research and development projects focused on electro-hydraulic actuators are performed. Currently he is leading a research project for the development of new diagnostic methods and collaborative robotic assistance during repair process of aircraft components in accordance with aviation regulations.

Gerko Wende, graduated in Electrical Engineering at the University of Hannover in 1996 and received a PhD in 2003 from the Institute of Flight Guidance & Control at the Technical University of Braunschweig. He then continued working as a scientist and flight test engineer at the same University with a research focus on flight measurement systems and avionics. During this time he initiated an University Spin-Off in the framework of European Promotion of economic development. Since 2004 Gerko Wende is employed with Lufthansa Technik where he is currently the Head of the Innovation Management in the Product Division Component Services. At his previous activities at Lufthansa Technik he has been responsible for strategic product planning and research at the department of Original Equipment Innovation. From 2009 until 2012 Gerko Wende gave lectures at the Technical University of Hamburg in the topics of Flight Mechanics, Flight Test and Flight Measurement Systems.

Rocco Gentile, born in Barletta (Italy) in 1992, is a mechanical engineer and Ph.D. student in Mechanical Engineering at Politecnico di Torino, where he graduated in 2016. His scientific activity is focused in the area of advanced diagnostic and prognostic of hydraulic servo-actuators. In particular, his main activity is focused data-analysis and implementation of machine learning techniques in diagnostic field. He is member of the servo-systems and mechatronic

research group of the Department of Mechanical and Aerospace Engineering.

Francesco Marino, graduated in Aerospace Engineering at Politecnico di Torino works as research assistant since 2017. His research activities are focused on primary flight servo-actuators (hydraulic servo-systems), diagnostic, features engineering, deep learning and collaborative robots. Currently, he is mainly involved in a project in partnership with Lufthansa Technik, where leads research activities related to: data-analysis, predictive maintenance and automated maintenance procedures. He is member of the servo-systems and mechatronic research group.

Antonio Carlo Bertolino, born in Cagliari (Italy) in 1992, is a Ph.D. student in Mechanical Engineering and Research assistant in Applied Mechanics at Politecnico di Torino. He graduated in Mechanical Engineering at Politecnico di Torino in 2016. His research activity is focused in the area of aerospace applications, such as flight control systems for fixed and rotary wing aircrafts (hydraulic and electro-mechanical servo-systems) and their prognostics. In particular, his main interest is in the development of high-fidelity model of ball screws for EMA flight controls. He's a student member of ASME since 2017.

Andrea Raviola, he got his bachelor's degree in aerospace engineering in 2015 at the Polytechnic of Turin, while now he is attending his master's in mechanical engineering at the Polytechnic of Turin focusing in automation and production processes. Nowadays, he is writing his thesis about automation of primary flight control actuators maintenance procedures using collaborative robotics at Lufthansa Technik AG. His main interests are: industrial and collaborative robotics, human-robot interaction and cognitive architectures in robotics.

Giovanni Jacazio, full professor of Applied Mechanics and lecturer of control systems at Department of Mechanical and Aerospace Engineering, Politecnico di Torino, Turin, Italy, until 2015, now retired; he is lecturing courses on fly-by-wire flight control systems and PHM in the Doctoral School of Politecnico di Torino and consulting for high tech companies. His main research activities are in the areas of flight control systems for aerospace applications and of prognostics and health management. He has been Research Leader for several European and national research programs, Coordinator of research and consulting activities for several engineering industries. He is member of the SAE A-6 Committee on Aerospace Actuation Control and Fluid Power Systems, and fellow of the Prognostics and Health Management Society.